

15th International Cosmic Ray Conference

CONFERENCE PAPERS

VOLUME 5

SP SESSION



BULGARIAN ACADEMY OF SCIENCES

PLOVDIV, BULGARIA
AUGUST 13-26, 1977

ENERGY SPECTRUM OF FLARE PARTICLES FROM AN IMPULSIVE ACCELERATION PROCESS

J. Pérez-Peraza, M. Gálvez and R. Lara A.

Instituto de Astronomía,
Universidad Nacional Autónoma de México
México 20, D.F.

Abstract. Energy spectra of non-relativistic solar particles accelerated in neutral current layers and magnetic flux loops are derived from the establishment of particle motion equations within these configurations. The same general spectral shape is obtained for different current sheet configurations. Current disruption models furnish an inverse power law spectrum. Among the several current sheet models analysed, the best representation of solar particle spectra either of delayed or prompt events is given by the PRIEST'S configuration for both the coronal and chromospheric levels. The acceleration spectrum from the ALFVEN-CARLQVIST model may support better coronal production in delayed events.

1.-Introduction. The feasibility of a given flare theory which can describe the kind of phenomena most likely to occur at the source, may be evaluated by the rapidity of local energy conversion to flare energy within the time scale required, the appropriate spatial and temporal sequence of events, etc. Given that most of the optical and corpuscular manifestations of the flare phenomenon seem to be directly associated with solar suprathermal particles, we believe that the ability of a model to predict the adequate energy spectrum of particles is another useful tool to test flare models and to draw inferences about the physical conditions of flare regions. At present it is widely spread the concept that solar cosmic rays, Type IV and probably Type II bursts, appearing in some high energy prompt events, are generated in a second acceleration step of preliminarily accelerated particles. Impulsive events like hard x-rays and microwave bursts are attributed to a faster primary acceleration stage, narrowly associated with the local instability that triggers the flare process itself. The secondary acceleration which rises particles up to sub-relativistic and relativistic energies, in the way that is usually required in several flare theories (e.g. Wentzel 1963, 1964; Sturrock 1966, 1968; Sakurai 1965; Smith 1975), is attributed to a stochastic process (e.g. Pikelner and Tystovich 1975). The study of energy spectra of particles accelerated by a stochastic process has been previously attempted for Multi-GeV proton events (Pérez-Peraza and Galindo T. 1975 a, b). However, most of prompt events do not produce relativistic protons but a great amount of low energy particles. Thus, following the same line of work, we derive in this paper source energy spectra of non-relativistic particles generated in an impulsive primary process, where acceleration is mainly due to displacement currents or space charges rather than statistic fluctuating electric fields. Therefore, instead of solving a Fokker-Planck equation, as is usually made in cosmic ray physics (e.g. Tsytoich 1966; Heristchi *et al.* 1976) we have developed analytical expressions for the spectrum of flare particles from inherent features of each model. The analysis of energy spectra of the low energy component of prompt events may furnish fruitful information about the primary process of particle acceleration, the configuration and structure of the source, and thus to serve as a guide to discriminate among the several hypothetical assumptions of flare theories in order to delineate more realistic models. Concerning flare models, a considerable number of proposals have been developed, so that their examination may be done under different classifications: the energy source, the associated local instability, the magnetic field configuration, etc. (e.g. Schmidt 1969; Sakurai 1974; Svestka 1975). Since magnetic energy seems to be the most likely source of flare energy; we shall concentrate our analysis on flare models where the magnetic field plays the chief role. Following Svestka (1975) and Priest (1976) we can distinguish flare models in two categories according to the magnetic field configuration: (a) neutral current sheets, and (b) magnetic flux tubes. Therefore, analytical expressions for the differential energy spectrum of particles accelerated in these kind of configurations are obtained in this work and inter-comparison with experimental spectra will be reported elsewhere. In this preliminary approach we do not consider energy losses as in the previous work (Pérez-Peraza and Galindo 1975 b). Such a refinement must be introduced when the combined analysis of theoretical and observational spectra allows to select a promising candidate configuration.

2.- Energy spectrum from the acceleration region. The obtention of energy spectra of particles accelerated in a definite magnetic field configuration has been previously attempted in a numerical approach for the Petschek's model configuration (Friedman 1969), and analytically for the Syrovatsky's configuration (Bulanov and Sasarov 1975). Since the accelerating force proceeds from a Coulombian force field, the final energy distribution of particles depends on their random initial positions within the acceleration region. Thus according to Bulanov and Sasarov (1975), the differential energy spectrum by unit time and unit length of the configuration may be written as:

$$N(E)dEdZ = J_0 \left| \frac{dX_0}{dE} \right| dEdZ \quad (1)$$

where x_0 denotes the initial particle position and J_0 is the particle density by unit time flowing at the boundary of the acceleration region. The modulating factor $|dx_0/dE|$ of the local flux J_0 determines the manner, as particles once accelerated in a given configuration are distributed according to their final energies. Particles which spend more time in a region of constant electric field, or whose initial positions are pre-privileged within a region of varying electric potential, reach the highest energies and conversely. Therefore, it follows that in order to establish $|dx_0/dE|$ it is necessary to study the behaviour of particles in the electromagnetic field inherent to each model.

3.- General equations of particle behaviour in current sheets. The astrophysical problem of neutral current sheet configurations has been studied from several points of view: the energy dissipation process (homogeneous, by resistive instabilities, by a wave mode, etc.) the geometric configuration (open and closed sheets), stationary and non-stationary process, compressible and incompressible media, etc. We have limited our analysis to those solar models that propose a explicit magnetic field configuration, which turns generally necessary in antiparallel and hyperbolic topologies of opposite magnetic-fields to determine particle trajectories within the acceleration region (Table 1). This means that for some important flare models we have been unable to derive energy spectra (e.g. Sturrock 1966, 1968, etc.). The analysis of particle trajectories in this kind of configurations has been carried out by Aström (1956), and Weiss and Wild (1964); here we shall follow the procedure developed by Speiser (1965) and Bulanov and Sasarov (1975), to

Sweet (1958)- Parker (1963)	$B = [0, -\frac{x}{\delta} B_0, 0]$
Petschek (1964)- Friedman (1969)	$B_I = (-2M_0 B_0, -B_0, 0)$ $B_{II} = (-M_0 B_0, 0, 0)$ $B_{III} = (-3M_0 B_0, -B_0, 0)$ $B_{IV} = [-M_0 B_0 (1 + x /\delta), (-x/\delta) B_0, 0]$ $B_V = [-M_0 B_0 (2 + x /\delta), (-x/\delta) B_0, 0]$
Syrovatsky (1966, 1974)	$B = B_0 (-y, -x, 0)$
Coppi-Friedland (1971)	$B = [(v a_2 / c_0 \delta) B_0, (v(1+a_2)/c_0 \sigma) B_0, 0]$ $a_2 = 1, c_0 = \text{sound velocity}$
Yeh-Axford (1970)	$B = -\frac{\sigma E}{2c^2} (B_x, B_y, 0)$ $B_x = (1 + 1/\cos 2\beta) Y$ $B_y = (-1 + 1/\cos 2\beta) X$ $\beta = 65^\circ$
Sonnerup (1970)	$B_x = B_1 [6.7 (\frac{Y}{L})^2 + b_3 (\frac{Y}{L})^3 + c_5 (\frac{Y}{L})^5]$ $B_y = B_1 [6.7 (\frac{X}{\delta})^2 + b_3 (\frac{X}{\delta})^3 + b_5 (\frac{X}{\delta})^5]$ $L = (1 + (2)^{1/2} v \delta / v) ; c_5, b_3, b_5 \text{ and } b_5 \text{ are constants.}$
Priest (1973)	$B = [(2B_1/L) Y, (B_0/L) X, 0]$
Smith-Raadu (1972)	$B = (B_0, -(B_0/L) X, 0)$
Priest-Raadu (1975)	$B = (0, -B_0(t) \text{sen}[\pi X / 2\delta(t)], 0)$ $B_0(t) = c t e^{-\gamma t^2}$ $1 \leq \gamma \leq 2$

Table 1.- Magnetic field configurations of different models; B_0 is the input magnetic field strength into the diffusion region, B_1 the emergent field after reconnection; δ is the half-width and L the length of the sheet. $M_0 = v/V$ with v and V the diffusion and Alfvén velocities respectively. The induced electric field is given by \vec{E} .

where the energy due to cyclotronic velocities has been neglected. The time t' can be obtained from the circular drift in the XY plane when the particle is at the boundary of the sheet of radius δ

$$X^2(t') + Y^2(t') = \delta^2 \tag{8}$$

derive analytical expressions of the motion equations. Let us consider the individual behaviour of particles; therefore, the electromagnetic force acting on particles is given by the Lorentz equation:

$$\vec{F} = e(\vec{E} + \frac{1}{c} \vec{u} \times \vec{B}) \tag{2}$$

where e is the electronic charge, c the light velocity and u is the particle velocity. $\vec{E} = (1/c) \vec{v} \times \vec{B}$ is the electric field which in current sheets appears mainly from spatial variations of the magnetic field $\vec{B} = (B_x, B_y, 0)$ when field lines diffuse inward with velocity v ; thus, according to Faraday and Gauss laws \vec{E} is a constant. At time $t=0$, before field line diffusion occur, particles have initial positions $(X_0, Y_0, 0)$ within the sheet and the velocity of the local plasma. Once diffusion starts the general particle motion equations are from Eq. (2)

$$\ddot{X} = (-e/mc) Z B_y \tag{3}$$

$$\ddot{Y} = (e/mc) Z B_x \tag{4}$$

$$\ddot{Z} = (e/m) E + (e/mc)(\dot{X} B_y - \dot{Y} B_x) \tag{5}$$

integration of (5) gives

$$\dot{Z} = (e/m) E t + F \tag{6}$$

where the contribution of the magnetic field components is represented by $F = F(X, Y, X_0, Y_0, B_0, D)$ with D denoting the geometrical dimensions of the sheet. It is systematically found that F becomes negligible with respect to the first term of (6) while t increases as we shall illustrate later for the Sweet-Parker model, where the sheet dimensions are the largest. After an elapsed time t' particles leave the diffusion region with a final energy:

$$E = (m/2) (\dot{X}^2 + \dot{Y}^2 + \dot{Z}^2) \approx \frac{e^2 E^2}{2m} t'^2 \tag{7}$$

to evaluate $X(t')$ and $Y(t')$ it can be seen that given the shape of configurations of Table 1, the substitution of (6) in (3) and (4) leads to the following kind of relations

$$\ddot{X} = \pm C X t; \quad \ddot{Y} = \pm C Y t \quad (9)$$

where C is a constant which differs according to the model configuration. The solution of a equation of type $\ddot{X} \pm C X t = 0$ may be obtained by performing the following variable changes $C = T^{-3}; R(t) = t/T, X = R^{1/2} s$ and $\omega = (2/3)R^{3/2}$, leading to a differential equation of the form $\omega^2(d^2s/d\omega^2) + (ds/d\omega) : (\omega^2 + 1/9)s = 0$ which solution is a Bessel function of order $(-1/3)$, either of an ordinary or modified kind, according to the sign of its third term; i.e., depending on whether the field components (Table 1) are taken negative or positive with respect an established origin, the solution is given by the modified or the ordinary function respectively, such that evaluated under boundary conditions ($X=X_0$ at $t=0$) we have $X(t) = X_0 p R^{1/2} J(\omega)_{-1/3}$ or $X(t) = X_0 p R^{1/2} I_{-1/3}(\omega)$, with $p = \Gamma(2/3) 3^{1/3}$. The solution of order $(-1/3)$ is preferred to the solution of order $(1/3)$ because it entails a longer duration of particles within the region where acceleration takes place. Since we are interested in the behaviour of particles in the diffusion region as time elapses, the asymptotic behaviour of Bessel functions as t increases is considered

$$I_{-1/3}[2/3(t/T)^{3/2}] = \frac{e^{-\pi/4} i^2 \exp[2/3(t/T)^{3/2}]}{(\pi/3)^{1/2} (t/T)^{3/4}}; \quad J_{-1/3}[2/3(t/T)^{3/2}] = \frac{\cos[2/3(t/T)^{3/2} - \pi/12]}{(\pi/3)^{1/2} (t/T)^{3/4}} \quad (10)$$

		δ (cm)	v (cms ⁻¹)	E_0 (eV)
Sweet-Parker	Incomp.	$(c/0.87) (L/4\pi v)^{1/2}$ = 5.2×10^3	$(c/0.87) (v/4\pi \sigma L)^{1/2}$ = 1.8×10^3	$[(eB_0 c^2 / (0.87)^3 4\pi \sigma) (v/4\pi \sigma L)^{1/2}] m^{1/3}$ = 0.19
	comp.	$(cL/B_0) [n_0 / \sigma L (3mkT_e)^{-2}]^{1/2}$ = 5.4×10^2	$[(B_0^2 / 48\pi^2 n_0 \sigma L) (3/mkT_e)^{-2}] c^{1/2}$ = 1.3×10^4	$(eB_0^2 c^2 / 48\pi^2 \sigma [(3/mkT_e)^{-2} (3/n_0 \sigma L)^{1/2}]^{2/3} m^{1/3}$ = 0.61
Patschek	incomp.	$c^2 / 0.4\pi v \sigma$ = 0.207; $\alpha = 0.2$	0.1V = 3.45×10^7	$(0.1eB_0 c v / 4\pi \sigma)^{2/3} m^{1/3}$ = 116.9^0
	comp.	$(1+\alpha) c^2 / 0.8\pi v \sigma$ = 0.124; $\alpha = 0.2$	0.2V / (1+ α) = 5.75×10^7	$(0.2ecB_0 v / 4\pi (1+\alpha)\sigma)^{2/3} m^{1/3}$ = 164.4
Covari-Brovat-Sky	comp.	$4\pi M n_0 / B_0^2 (3kT_e / M) (1+T_i / T_e)$ = 0.385	$\frac{B_0^2 c^2}{16\pi^2 m \sigma n_0 (3kT_e / M) (1+T_i / T_e)}$ = 1.8×10^7	$(ecB_0^3 M / 16\pi^2 m \sigma n_0 3kT_e (1+T_i / T_e))^{2/3} m^{1/3}$ = 77.3
	Comp.	Arbitrary value: 100	Arbitrary value: 10	$(e^2 v B_0 c / 4\pi \sigma_c)^{2/3} m^{1/3}$ = 31.36 $\sigma_c = 10^5$ s
Yeh-Axford	incomp.	$c^2 / 2.41v \sigma$ = 0.107	2.41V = 8.34×10^8	$(4.82ec^2 B_0 / 4\pi \sigma [(1/\cos 2\theta) - 1])^{2/3} m^{1/3}$ = 8.01×10^8
Sonnerup	incomp.	$>(1/eB_0) (mkT_e / 5)^{1/2}$ = 8.9×10^{-12}	0.059V = 2.03×10^7	$(2.41VeB_0 v c / 4\pi \sigma c_1)^{2/3} m^{1/3}$ = 3.0×10^{-8} $c_1 = 6.7$
Friest-Raadu	Incomp.	$c^2 / 0.715v \sigma$ = 0.363	0.057V = 1.96×10^7	$(3.25 \times 10^{-3} eLB_0 v^2 / 2c)^{2/3} m^{1/3}$ = 9.94×10^7
Priest-Raadu	incomp.	Arbitrary value: 1	Arbitrary value: 10 ⁸	$(\delta e v^2 B_0 / c)^{2/3} m^{1/3}$ = 1.37×10^3
	incomp.	Arbitrary value: 1	Arbitrary value: 10 ⁸	$(2eB_0^2 v^2 \delta (1+\gamma^2/2) / c t e \pi c)^{2/3} m^{1/3}$ = 6.41×10^4 $\gamma = 1.5$

Table 2 The spectrum parameters for incompressible and compressible flare models: $v = B_0 / (4\pi m_p)^{1/2}$ is the Alfvén velocity; m and M are the proton and electron mass respectively T_i and T_e are the ionic and electronic temperatures respectively ($T_i / T_e = 0.1$); k is the Boltzman constant.

* The constant has been arbitrarily chosen as unit.

However, when the field configuration has components which are null or constants the solution of (3) and (4) takes the trivial forms $X(t') = Vt + X_0$, or $X(t') = (C/6)t^3 + Vt + X_0$ where V is the Alfvén velocity. Since the exponential of time increases faster than either a cubic function of time or a trigonometric function of time, the solution of (3) or (4) is basically given by the modified Bessel function, which is also true when perturbations in the position appearing from perturbations in the magnetic field are considered, as in the model of Sonnerup (1970). This leads systematically to found that one of the left terms in Eq. (8) is negligible with respect to the other one, so that the following expression for the time is generally obtained.

$$t' \approx T \{ 1.5 \ln [(\pi^{1/2} / \Gamma(2/3)) e^{-\pi/4} 3^{1/6} (\delta / X_0)] \}^{3/2} \quad (11)$$

with the exception of regions II and III of Petschek's current sheet where acceleration is provided by fluctuating electric fields. Therefore from (7) the particle energy when it leaves the acceleration region is $E = (e^2 \epsilon^2 T^2 / m) [0.89 \ln 1.36 (\delta / X_0)]^{4/3}$ and thus

$$X_0 = 1.36 \delta \exp[-1.12 (E/E_0)^{3/4}] \tag{12}$$

where $E_0 \approx e^2 \epsilon^2 T / m$ is a characteristic energy, which value depends on inherent features of each model. Taking the derivate of (12) and introducing it in (1) a general expression for the differential spectrum of particles accelerated in current sheets is obtained

$$N(E) dEdZ = A (E/E_0)^{-1/4} \exp[-1.12 (E/E_0)^{3/4}] dEdZ \tag{13}$$

where $A \approx K n v \delta / E_0$, with $K = \pi^{1/2} e^{\pi/12} / \Gamma(2/3) 2^{1/4} 3^{1/6} = 1.1436$. It is then clear that the current density $J_0 = n v$ depends on individual model through the incoming velocity and on the compressibility or incompressibility of the plasma sheet. For the incompressible case we have considered the local density (i.e., $n = n_0$). In Petschek's model particles are effectively continuously accelerated in regions II to V, two or which are the superposition of adjacent configurations. Among these configurations, three of them are populated by fluctuating electric fields and stochastic acceleration becomes predominant in two regions. If the electric field is considered as roughly constant within the regions of magnetic discontinuities, the particle energy spectrum from Petschek's configuration takes the following form

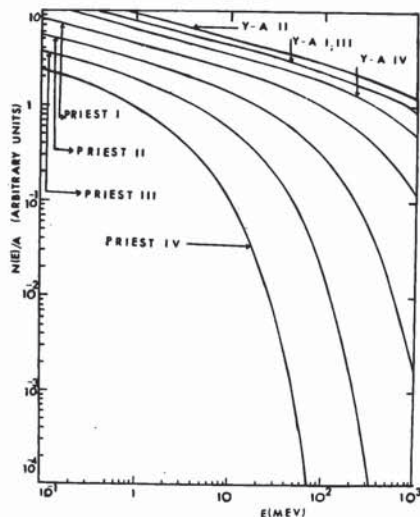
$$N(E) dEdZ = A \{ (E/E_0)^{-1/2} \exp(-2.24 (E/E_0)^{3/4}) + (E/E_0)^{-1/4} \exp[-1.12 (E/E_0)^{3/4}] \} dEdZ \text{ (diffusion regions)}$$

$$N(E) dEdZ = [(2/m) E^{-1/2} + (B_0^2 / 2e^4 \epsilon^4)^{1/2} E^{1/2} + 1] dEdZ \text{ (stochastic regions)} \tag{14}$$

it follows from (13) or (14) that the evaluation of energy spectra of particles accelerated in current sheets require the characteristic values δ , v and E_0 that we have summarized in Table 2 for the incompressible and compressible cases for an arbitrary set of parameters: $n = 10^{11} \text{ cm}^{-3}$, $B = 500 \text{ gauss}$, $\sigma = 10^{13} \text{ s}^{-1}$, $T_e = 10^5 \text{ K}$ and $L = 10^9 \text{ cm}$. As can be seen from the characteristic value E_0 (Table 2), with the exception of the Priest and Yeh-Axford models, expressions (13) and (14) are not able to describe solar particles, because at $E < 1 \text{ KeV}$ there is an extremely abrupt fall of many decades in particle intensity in an energy decade, becoming practically null at higher energies. A similar behaviour is obtained varying $n = 10^9 - 10^{13} \text{ cm}^{-3}$, $B = 100 - 500 \text{ gauss}$, $T_e = 10^5 - 10^7 \text{ K}$ and $\sigma = 10^{13} - 10^{17} \text{ s}^{-1}$. Therefore, we have illustrated in Fig. 1 the behaviour of energy spectra obtained with the two models that seems to be valuable in describing solar particles (Yeh-Axford and Priest models). On Table 3 we have summarized the relevant parameters of spectra in Fig. 1, together with $E_{\text{max}} = eEL = (e/c)vBL$ in each case. It must be mentioned, however, that the Priest-Raadu model may also give a valuable spectrum for $\delta > 10 \text{ cm}$ and $v > 10^8 \text{ cm s}^{-1}$. For the rest of models analysed in this work, we should assume a turbulent conductivity $\sigma \approx 10^5 \text{ s}^{-1}$, $B > 500 \text{ gauss}$ and $L > 10^9 \text{ cm}$ in order to obtain a valuable description of solar particle spectra.

	I	II	III	IV
$n (\text{cm}^{-3})$	10^{10}	10^{11}	10^{12}	10^{13}
δ (cm)	3.4×10^{-3}	0.107	0.341	1.07
v (cm s ⁻¹)	2.6×10^9	8.3×10^8	2.6×10^8	8.3×10^7
E_0 (MeV)	3.7×10^3	8.0×10^3	3.7×10^3	1.7×10^3
A (cm s eV) ⁻¹	2.7×10^7	1.28×10^9	2.7×10^{10}	5.9×10^{11}
E_{max}	1.3×10^4	4.0×10^3	1.3×10^3	417.0
δ (cm)	1.1×10^{-2}	0.363	1.15	3.63
v (cm s ⁻¹)	6.2×10^7	1.9×10^7	6.2×10^6	1.9×10^6
E_0 (MeV)	461.0	99.4	21.4	4.6
A (cm s eV) ⁻¹	1.5×10^7	8.2×10^9	4.7×10^{11}	1.7×10^{13}
E_{max} (GeV)	311	98	31	9.8

Table 3. The Priest and Yeh-Axford spectra parameters for $B = 500 \text{ gauss}$; $L = 10^9 \text{ cm}$, $\sigma = 10^{13} \text{ s}^{-1}$. Set I is given with $\sigma = 10^{14} \text{ s}^{-1}$.



4.-Magnetic flux tubes. Among the magnetic flux loops models of flares there are several fundamental differences concerning the energy storage process, the basical configuration (force-free twisted tubes or sheared force free fields, e.g., Svestka 1975) we have analysed those models where the impulsive electromagnetic field is given explicitly, therefore, disregarding models where acceleration is performed by fluctuating electric fields (e.g., Wentzel 1964; Sakurai 1965;

Pnewman 1967; Piddington 1974). One of the most popular concepts in flux loop models is electric current disruption in the solar atmosphere (Heyvaerts 1974), as for instance the model proposed by Alfven and Carlqvist (1967), and Carlqvist (1969) where the space charge region for particle acceleration is assimilated to a vacuum diode. Let us discuss the particle spectrum from this model: since the problem is considered one-dimensional, the potential difference in the space charge region may be expressed as $U = DZ^{2/3}Z^{4/3}$, with $D = 1.6 \times 10^{-7} n_0^{2/3}$ (M.K.S.). Assuming that the initial velocities $\dot{Z}_0 \approx 0$, we obtain from the energy conservation law that particles leave the acceleration region with velocity $Z = (2eD/m)^{3/4} Z$, where $Z = d - Z_0$ is the traversed distance of particles with initial position Z_0 to leave the space charge region of length d . Therefore the final energy of particles is $E = (2/m)^{1/2} (Ke)^{3/2} (d - Z_0)^2$ and thus $(dZ_0/dE) = 1.3 \times 10^{12} n_0^{-1/2} E^{-1/2}$; making use of the boundary flux furnished by the model $J_0 = (2e/m)^{1/2} (0.826 \epsilon_0 e d^2) U_{Z=d}^{3/2} = 1.14 \times 10^7 n_0^{3/2}$, we obtain from Eq. (1)

$$N(E) dE dZ = A E^{-1/2} dE dZ \quad (\text{cm}^{-1} \text{s}^{-1} \text{eV}^{-1}) \quad (15)$$

where $A = 2.35 \times 10^{-4} n_0$. The high energy cutoff of this model when $Z_0 = 0$ and $d = 2 \times 10^6$ cm is $E_{\text{max}} = 3.74 \times 10^2 n_0$ (eV); therefore, it follows that either $n_0 \leq 10^7 \text{cm}^{-3}$ or $d < 2 \times 10^6$ cm at the solar source. Assuming that the same instability and space charge region may occur within the loop configuration proposed by Heyvaerts (1974), a similar spectral shape to (15) is obtained. In fact, due to the low conductivity perpendicular to the field lines, a right path of particles may be assumed and thus the energy conservation law is enough to derive the energy distribution of the accelerated particles. Other interruption circuit models as those of Takakura (1971) and Kaburaki (1975) leads also to spectral shapes of the form νE^{-Y} , when the potential and electric fields are transformed to depend on the radial coordinates of the current filaments. However these two models are mainly important in the production of low energy particles: i.e., in the Takakura's model we have $E_{\text{max}} = 1.3 \times 10^{-8} (n_i/T_e) d$ (eV), such that taking the model parameter $d = 4 \times 10^7$ cm, we obtain in the corona ($n_i/T_e = 10^{10}$) $E_{\text{max}} \approx 5.2$ KeV and $E_{\text{max}} \approx 5.2$ MeV in the chromosphere ($n_i/T_e \approx 10^{13}$); whereas in Kaburaki's model $E_{\text{max}} = 7.7 \times 10^{-10} (Tn_0)^{1/2} d$ (eV) with $d = 5.9 \times 10^7 n_0^{1/4}$ (cm), such that for $n_0 \approx 10^{10} \text{cm}^{-3}$ and $T = 10^6$ K, $E_m \approx 14$ KeV, and even lower in the chromosphere. Nevertheless these models may be considered in relation with the thermal phase of flares, where the particle spectrum may only be indirectly known from the electromagnetic radiation emitted. Another flux loop configuration of considerable interest is that of Gold and Hoyle (1960) model, however due perhaps to the fact that the electric field in the interpenetration region is not always constant, we have obtained an incongruous spectral distribution. The problem is in reconsideration and results will be reported elsewhere.

5-Discussion. In spite of the rough approximations carried out to obtain the particle trajectories and acceleration time, we have derived energy spectra from an impulsive process in current sheets which have similar shape than that obtained from a stochastic process by solving a Fokker-Planck equation (Pikelner and Tystovich 1975), as $N(E) \sim (E/E_0)^{-Y_1} \exp(-Y_2(E/E_0)^{Y_3})$, differing in the values of Y_1, Y_2 , and Y_3 . Therefore it can be drawn from this preliminary analysis, that particles accelerated in neutral current layers leave the source with a spectral distribution of the general shape shown above. Concerning the kind of approximations performed through this work, let us discuss the negligence of the second term at right in Eq. (6), taking as illustration the Sweet-Parker model. In this case, Eq. (6) may be rewritten as $\dot{Z} = (e/m)[\epsilon t + B_0/2c\sigma](y^2 - y_0^2)$ where $\epsilon = (B_0/c)[c(V/2\sigma)^{1/2}]$ is such that taking the extreme supposition of $x^2 - x_0^2 \approx \delta^2$, Eq. (6) may be reduced to $\dot{Z} = B_0(V/L\sigma)^{1/2}(t + L/2V)$. Therefore it can be seen that it is enough to consider times > 5 s (for $B = 500$ gauss, $L \leq 10^9$ cm and $n_0 \leq 10^{12} \text{cm}^{-3}$) to justify the mentioned approximation. In relation with the conclusions that can be obtained from this preliminary analysis, we believe that they can be discussed in terms of the parameters E_0 and E_{max} (Tables 2 and 3): according to the values of σ and L used in our evaluations, the field configuration which seems to be the more appropriate to describe solar particle production is that of the Priest model when $n_0 > 10^{12} \text{cm}^{-3}$; although the value of E_0 for $n_0 \approx 10^{11} - 10^{12} \text{cm}^{-3}$ may be considered as typical observational values, the predicted E_{max} value is very high in comparison with observational evidences (Heristchi et al. 1976). The same argument may be extended to the Yeh-Axford model, added to the fact that the E_0 values are extremely far above the observational values. However, it is clear that a reduction in the value of σ and L would lead to reasonable values of E_0 and E_{max} ; at any event, with regard to E_0 this model would be operative only at chromospheric levels ($n_0 \geq 10^{13} \text{cm}^{-3}$), and with regard to E_{max} , the value of L should be reduced to $L \leq 10^7$ cm to explain only high energy particle events. Turning back to the more promising configuration (Priest 1973), which spectrum does not depend explicitly on temperature, but basically on (B, L, n_0) , it can be seen from Table 1 that from the point of view of the parameter E_0 , the spectrum is able to describe non-relativistic events when $n_0 \geq 10^{11} \text{cm}^{-3}$, however this is not true with regard to E_{max} in which case L should be reduced to $10^7 - 10^8$ cm to explain only high energy spectra. For lower densities ($n_0 = 10^9 - 10^{10} \text{cm}^{-3}$) in addition to the consideration of taking L quite lower, the field must be weaker

($B \leq 100$ gauss) in order to describe high energy prompt events. In order to describe delayed events (low energy particles) L should be reduced to $\sim 10^6$ cm for $B \leq 100$ gauss and $n \leq 10^{10}$ cm^{-3} or alternatively $B \approx 500$ gauss with $n \geq 10^{11}$ cm^{-3} . Therefore this model seems to be operative at both chromospheric and coronal levels for both non-relativistic prompt events and delayed events. Examination of Fig. 1 shows that acceleration in current sheets can explain particle production in Multi GeV events if acceleration occurs in a high density medium ($n_0 \geq 10^{11}$ cm^{-3} in the Priest's configuration), whereas a very high density $n_0 \geq 10^{13}$ cm^{-3} must be assumed in the Y-A model. In fact Bulanov and Sasarov (1975) predict a very flat spectrum for relativistic particles accelerated in neutral layers. Therefore, because the scarcity of Multi-GeV events we prefer the picture of acceleration at coronal levels, with isotropic injection, such that occasionally when the appropriate conditions exist, reacceleration at chromospheric levels by a stochastic process rises particles up to relativistic energies. With regard to flux tube models we infer from section 5, that these configuration may be easily associated with particle acceleration in delayed events (e.g. recurrent events, where typical spectra are very flat); for the time being a deep analysis is performed and results will be reported posteriorly.

REFERENCES

- Alfven and Carlqvist, P. 1967 Solar Phys., 1, 220
 Astrom, E. 1956 Tellus 8, 260
 Bulanov, S.V. and Sasarov, P.V. 1975 Sov. Astron. 19, 464
 Carlqvist, P. 1969 Solar Phys., 7, 377
 Coppi, B. and Friedland, A.B. 1971 Ap. J. 169, 379
 Friedman, M. 1969 Phys. Rev. 182, 1408
 Gold, T. and Hoyle, F. 1960 M.N.R.A.S. 57, 253
 Heristchi, Dj; Trotter, G. and Pérez-Peraza, J. 1976 Solar Physics 49, 151
 Heyvaerts, J. 1974 Solar Phys., 38, 419
 Kaburaki, O. 1975, Publ. Astron. Soc. Japan 27, 45
 Parker, E.N. 1963 A.J. Suppl. (77) 8, 177
 Pérez-Peraza and Galindo, J. 1975a Rev. Mex. Astron. Astrof. 1, 3
 Pérez-Peraza, J. and Galindo, J. 1975b 14th International Cosmic Ray Conference 5, 1557
 Petscheck, H.E. 1964 Proc. AAS-NASA Symp. 50 Phys. of Solar Flares (Goddard Space Flight Center, Greenbelt Md.)
 Piddington, J.H. 1974, Solar Phys., 38, 465
 Pikelner, S.B. and Tsytoich, V.N. 1975 Sov. Astron. 19, 450
 Pneuman, G.W. 1967 Solar Phys., 2, 462
 Priest, E.R. 1973 Ap. J. 181, 227
 Priest, E.R. and Raadu, M.A. 1975 Solar Physics 43, 177
 Priest, E.R. 1976 Proc. of the International Symp. on Solar Terrestrial Physics (Boulder Co) 1, 144
 Sakurai, K. 1965 Rep. Space Res. Japan 19, 408
 Sakurai, K. 1974 Physics of Solar Cosmic Rays, University Tokyo Press
 Schmidt, H.U. 1969 Solar Flares and Space Research, p. 331, ed. by C.D. Jager and Z. Svestka
 Smith, D.F. and Raadu, M.A. Cosmic Electrodynamics 3, 285
 Smith, D.F. 1974 I.A.U. 57, 253
 Sonnerup, B.U.O. 1970 J. Plasma Physics, 4, 161
 Speiser, T.W. 1965 J. Geophys. Res. 70, 4219
 Sturrock, P.A. 1966 Nature 211, 695
 Sturrock, P.A. 1968 I.A.U. Symp. 35, 471
 Sweet, P.A. 1958 Nuovocimento Supp. 8, Ser. 188
 Syrovatsky, S.I. 1966 Sov. Astron. 10, 2
 Syrovatsky, S.I. 1974 Tr. Fiz. Inst. Akad. Nauk. SSSR, 74, 3
 Svestka, Z. 1976 Solar Flares; Geophys. and Astrophys. Monographs. Reidel Publish. Co.
 Takakura, T. 1971 Solar Phys. 19, 186
 Tsytoich, V.N. 1966 Sov. Phys. Uspekhi, 9, 370
 Wentzel 1963 Ap. J. 135, 137
 Wentzel 1964 AAS-NASA-50 Symp. on the Physics of Solar Flares, p. 397 and Ap. J. 140, 1563
 Weiss, A.A. and Wild, J.P. 1964 Aust. J. Phys. 17, 282
 Yeh, T. and Axford, W.I. 1970 J. Plasma Physics 4, 207